Dielectric and electrical properties of nematic liquid crystals 6CB doped with iron oxide nanoparticles. The combined effect of nanodopant concentration and cell thickness

O.V. Kovalchuk [a,b,c,*], T.M. Kovalchuk [d], N. Tomašovičová [e], M. Timko [e], K. Zakutanska [e], D. Miakota [e,f], P. Kopčanský [e], O.F. Shevchuk [g], Y. Garbovskiy [h,*]

[a] Kyiv National University of Technologies and Design, 2, Nemirovich-Danchenko str, 01011 Kyiv, Ukraine
[b] National Technical University of Ukraine "Igor Sikorsky Kyiv Polytechnic Institute", 37, prospect Peremohy, 03056 Kyiv, Ukraine
[c] Institute of Physics, NAS of Ukraine, 46, prospect Nauky, 03680 Kyiv, Ukraine
[d] V. Lashkaryov Institute of Semiconductor Physics, NAS of Ukraine, 41, prospect Nauky, 03680 Kyiv, Ukraine
[e] Institute of Experimental Physics, Slovak Academy of Sciences, 47, Watsonova str, 04001 Košice, Slovakia
[f] Taras Shevchenko Kyiv National University, 64, Volodymyrska str, 01601 Kyiv, Ukraine
[g] Vinnytsia National Agrarian University, 3, Soniachna str, 21008 Vinnytsia, Ukraine
[h] Department of Physics and Engineering Physics, Central Connecticut State University, New Britain, CT 06050, USA

ARTICLE INFO

ABSTRACT

Dispersing nanomaterials in liquid crystals has emerged as a very promising non-synthetic way to produce advanced multifunctional and tunable materials. As a rule, dielectric and electrical characterization of such materials is performed using cells of single thickness. As a result, the published reports vary even for similar systems. Confusion still exists as to the effects of nanodopants and cell thickness on the dielectric and electrical properties of liquid crystals. This factor hinders a widespread use of liquid crystals - nanoparticles systems in modern tech products. In this paper, we report systematic experimental studies of the combined effect of the cell thickness and iron oxide nanoparticle concentration on the electrical and dielectric properties of nematic liquid crystals 6CB. The measured dielectric spectra can be divided into three distinct regions corresponding to a low frequency (<10 Hz) dispersion, dispersion free range (10^2 – 10^4 Hz (electrical conductivity) and 10^2 – 10^5 (dielectric permittivity)), and high frequency dispersion (10^4 – 10^6 Hz (electrical conductivity) and 10^5-10^6 Hz (dielectric permittivity)). The real part of the dielectric permittivity is not affected by the cell thickness and its value can be tuned by changing the concentration of nanoparticles. At the same time, the electrical conductivity depends on both cell thickness and nanoparticle concentration. At intermediate frequencies (10^2 – 10^4 Hz) the electrical conductivity obeys the Jonscher power law and is dependent on the cell thickness because of ion-releasing and ion-capturing effects caused by nanoparticles and substrates of the cell. In addition, its value is affected by the electronic conductivity due to iron oxide nanoparticles and their nanoclusters. At higher frequencies (10^4 – 10^6 Hz) the electrical conductivity follows a super linear power law and is nearly independent of the cell thickness and nanoparticle concentration.

© 2022 Elsevier B.V. All rights reserved.

1. Introduction

Numerous display and non-display applications of liquid crystals rely on electric field induced reorientations of their director

[1–5]. Orientation transitions in liquid crystals depend on their dielectric anisotropy [6]. In addition, such transitions can also be altered by the presence of ions in liquid crystals [6,7]. Therefore, measurements of dielectric and electrical properties of mesogenic materials are a standard part of their material characterization [6–8].

Future progress in liquid crystal science and technology strongly depends on the development of new liquid crystalline materials [9]. A very promising approach to create new mesogenic materials involves mixing liquid crystals with nanoparticles

* Corresponding authors at: Department of Physics and Engineering PhysicsCentral Connecticut State University1615 Stanley StreetNew Britain, CT 06050 USA. Tel.: +Phone: 860-832-2944

E-mail addresses: akoval@knutd.com.ua (O.V. Kovalchuk), ygarbovskiy@ccsu.edu (Y. Garbovskiy).

[10,11]. This interdisciplinary field is characterized by a very high level of research activity [10–12]. Physical properties of liquid crystals doped with nanomaterials of different origin were studied by many independent research groups around the globe. It was found that nanomaterials mixed with liquid crystals can improve their dielectric [13,14], electrical [14,15], optical and electro-optical [16–18], nonlinear-optical [19], viscoelastic [20], and thermodynamic properties including phase transition temperatures [21]. Additional references to original publications can be found in review papers on liquid crystals doped with magnetic [22,23], ferroelectric [24], semiconductor and dielectric [25,26], carbon-based [27,28], and metal [29] nanomaterials.

As was already mentioned, dielectric properties of liquid crystal materials are very important because they enable applications of liquid crystals relying on orientation transitions under the action of electric fields [1–6]. Even low concentrations of nanoparticles can significantly modify the dielectric properties of liquid crystals as was recently reported for liquid crystal systems doped with ferroelectric [30–36], superionic [37–39], carbon-based [40–45], magnetic [46–49], semiconductor [50–55], and metal [56–58] nanomaterials. Dielectric spectroscopy is a versatile experimental technique that allows measurements of complex dielectric permittivity over a wide range of frequencies [59–61]. As a result, both dielectric constants and electrical conductivity of liquid crystals doped with nanoparticles can be found [7,8,15,61,62].

Because of the complexity of the studied materials, experimental results reported even for similar systems vary both quantitatively and qualitatively [63,64,65] and references therein]. Many factors can affect the measured values of dielectric constants and electrical conductivity of liquid crystals doped with nanomaterials. Among them, the quality of alignment and the presence of ions in liquid crystals are of utmost importance. Ions in liquid crystals can interact with both nanopodants and substrates (alignment layers) of a liquid crystal cell. Such interactions are very important in the case of relatively thin cells [66–68]. They can result in the dependence of the direct current (DC) electrical conductivity of liquid crystals on the cell thickness [69,70]. At the same time, the use of thicker cells can lead to a lower alignment quality of liquid crystals thus affecting the measured values of both electrical conductivity and dielectric constants which are essentially anisotropic quantities.

As a rule, dielectric and electrical properties of liquid crystals doped with nanomaterials are studied using cells of the same thickness and by varying the concentration of nanoparticles. Several experimental reports indicate that electrical conductivity of plain (undoped) liquid crystals depends on the cell thickness [44,69,71,72]. In addition, recently performed analysis suggests strong dependence of the DC electrical conductivity of liquid crystals doped with nanoparticles on the cell thickness [66–68,70]. At the same time, systematic experimental studies of the combined effect of the cell thickness and nanoparticle concentration on the dielectric and electrical properties of liquid crystals doped with nanomaterials are still missing. Experimental studies of this combined effect are a major goal of our paper. More specifically, we study the effect of the iron oxide nanoparticle concentration and the effect of the cell thickness on the dielectric and electrical properties of nematic liquid crystals 6CB.

2. Materials and experimental methods

To study the combined effect of the cell thickness and nanodopant concentration on dielectric and electrical properties of nematic liquid crystals readily available materials were chosen. More specifically, a standard nematic liquid crystal 4-cyano-4′-hexylbiphenyl (6CB) was chosen as a mesogenic host and iron oxide nanoparticles – as nanodopants. The shape of iron oxide nanoparticles (NP) was nearly spherical. Their diameter was 5 nm. To reduce the aggregation of nanoparticles, they were coated with oleic acid and dispersed in chloroform. Nanoparticles were purchased from Ocean Nanotech.

The composites of thermotropic liquid crystal 6CB and iron oxide nanoparticles were prepared using the following procedure. The nanoparticles dispersed in chloroform were added to the liquid crystal in the isotropic phase. Subsequently, the mixture was stirred in the isotropic phase until the chloroform was evaporated. As a result, the composite with the concentration 0.1 wt% was prepared. Diluted samples, i.e., the samples with the concentrations 0.05 and 0.01 wt%, were prepared by adding an additional amount of liquid crystals. Before adding liquid crystals, as well as before each sample preparation for measurements, the composites were sonicated to eliminate the presence of aggregates.

Sandwich-like cells with homeotropic boundary conditions were used in our research. To reduce the impact of "edge effects", a cell was equipped with transparent measuring electrodes made of indium – tin oxide (ITO). To achieve a homeotropic alignment of 6CB nematic liquid crystals, ITO electrodes were covered with a thin polymer film. Homeotropic boundary conditions were chosen intentionally. Utilized nematic liquid crystals (6CB) have a positive dielectric anisotropy $\Delta\varepsilon$ (polarizability along the long axis of molecules is higher than that along the short axis, i.e., $\Delta\varepsilon > 0$) [73,74]. In the case of a planar liquid crystal cell, the applied external electric field leads to reorientation of planarly aligned mesogenic molecules along the field. As a result, to some extent the effect of the cell thickness and nanoparticle concentration can be masked by the electric field induced orientation transitions of a liquid crystal director. Even if the applied electric field is below the threshold value, the planar alignment of liquid crystals can become less perfect for thicker cells. As a result, the correct comparison of thin and thick cells will be compromised. To overcome these experimental challenges, cells with homeotropic boundary conditions can be utilized. In this case, the reduced quality of alignment for thicker cells can be mitigated by applying voltage that is greater than the threshold voltage of nematic liquid crystals. As a result, both thin and thick cells have nearly the same quality of homeotropic alignment.

The studies were performed at three different cell thicknesses d: 5, 20 and 50 μm. The thickness of the cell was set by spacers that were placed in between the guard electrodes.

Three different concentrations of iron oxide nanoparticles were used, namely 0.01, 0.05, and 0.1 wt%. Polarizing microscope observations revealed that the presence of even the highest concentration of nanodopants in liquid crystal does not influence the homeotropic orientation of LC molecules.

The measurements of dielectric and electrical properties of 6CB doped with iron oxide nanoparticles were carried out using a standard oscilloscopic method [61,75]. The amplitude of the applied sinusoidal voltage was 2.5 V. Measurements of the dielectric properties of the samples were performed within the frequency range $f = 6\ldots 10^6$ Hz at the temperature 293 K. Using the oscilloscopic method, we measured the values of the electrical resistance R and electrical capacitance C for individual frequencies, assuming that the equivalent circuit of the sample is the resistance and capacitance connected in parallel. Since we used the logarithmic scale to analyze the frequency dependences, the frequencies were chosen so that the interval between them on the logarithmic scale was the same.

According to the known geometric dimensions, the imaginary ε'' and real ε' components of the complex dielectric permittivity ε^* were determined based on the values of R and C, respectively

[61]. Also, Eq. (1), was used to determine the electrical conductivity σ of the studied samples at various frequencies (ε_0 is the vacuum permittivity):

$$\sigma = 2\pi f \, \varepsilon_0 \, \varepsilon'' \qquad (1)$$

The main conclusions were made by analyzing frequency dependences of ε', ε" and σ at different concentrations of nanoparticles and different sample thicknesses.

3. Results and discussion

3.1. Frequency dispersion regions of the real part of the complex dielectric permittivity

Fig. 1 shows the frequency dependence of the real part of the complex dielectric permittivity ε' for nematic liquid crystals doped with iron oxide nanoparticles (6CB + 0.01 % wt/wt NP) measured for three various cell thicknesses: 5 (1), 20 (2) and 50 μm (3). The dielectric spectra shown in this figure can be divided into three regions: **A** ($f < 10^2$ Hz), **B** ($10^2 < f < 10^5$ Hz), and **C** ($f > 10^5$ Hz). In the **B** region of the dielectric spectrum, the value of ε' does not depend on the frequency, and in the regions **A** and **C** it depends on the frequency, so it is logical to analyze the dielectric spectrum in each of these regions in greater detail.

3.2. The low-frequency dispersion of ε' (region A)

It is generally accepted that the low frequency dispersion of the real part of the complex dielectric permittivity is caused by the electrode polarization effect when the applied low frequency electric field results in the ion accumulation near the electrodes and the formation of electric double layers (EDL) [8,61]. The electrode polarization can also be accompanied with a charge transfer through the liquid crystal – electrode interface. As was shown in paper [61], in the case of homeotropic orientation of molecules, the low-frequency dispersion of the components of the complex dielectric permittivity ε' and ε" caused by charge transfer through the near-electrode region of the sample can be described by the Cole–Cole equation (2):

$$\varepsilon^* = \varepsilon_\infty + \frac{\varepsilon_S - \varepsilon_\infty}{1 + (i\omega\tau)^{1-\alpha}} \qquad (2)$$

where ε_s and ε_∞ are the values of the dielectric permittivity at the frequencies f = 0 and f = ∞, ω = 2πf is the angular frequency, τ is the dielectric relaxation time, and α is the Cole–Cole parameter.

To successfully apply Eq. (2) for the analysis of the charge transfer processes in liquid crystals, the frequency should vary within a wide range spanning several orders of magnitudes ($10^{-4} - 10^2$ Hz) [61]. Given limitations of the frequency generator used in our experiments, it was practically impossible to find the values of τ, ε_s and α for the studied samples because only a small part of the dependence ε"(ε') (i. e. Cole–Cole diagrams) was measured. An order of magnitude estimation of τ, ε_s and α using Eq. (2) was performed for the sample "6CB + 0.1 wt% NP" of the thickness 50 μm (for the chosen sample this could be made with the least error). Assuming that α = 0, it was found that τ = 0.13 ± 0.10 s, and ε_s = 2400 ± 2000. In addition, by following a procedure described in paper [61], the thickness W of the formed electrical double layer (EDL) was also estimated using Eq. (3):

$$W = \frac{d \, \varepsilon_s}{2\varepsilon_\infty}, \qquad (3)$$

Eq. (3) assumes that near each of the electrodes the electric double layers (EDL) with the same parameters are formed. As a result, for the chosen sample "6CB + 0.1 wt% NP" with the thickness 50 μm, the following value was found: W = 150 ± 130 nm.

3.3. The dispersion of ε' at intermediate (region B) and high (region C) frequencies

The real part of the complex dielectric permittivity does not depend on frequency in the region B ($10^2 – 10^5$ Hz, Fig. 1). In addition, it is independent of the cell thickness. (Fig. 1). At the same time, the value of ε' can be tuned by changing the concentration of iron oxide nanoparticles in nematic liquid crystals as shown in Fig. 2.

Experimental results shown in Fig. 2 suggest that even low concentrations of iron oxide nanoparticles can increase the value of a dielectric permittivity of nematic liquid crystal host. This result is consistent with existing reports for nematic liquid crystals doped with low concentrations of nanoparticles such as ferroelectric [31], zinc ferrite [47], carbon coated nanoparticles [48], etc. (additional references can be found in reviews [10,15,20]). Quantitatively, this increase can be described by applying recently developed models [10].
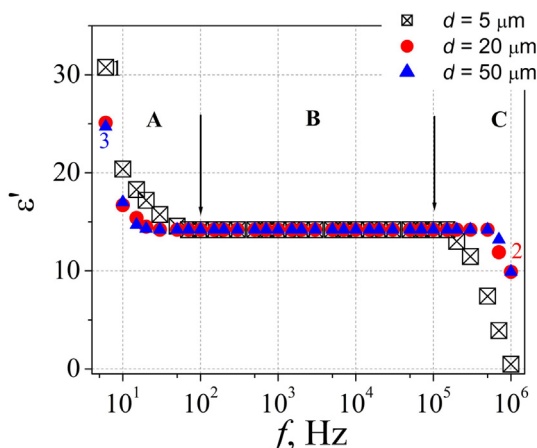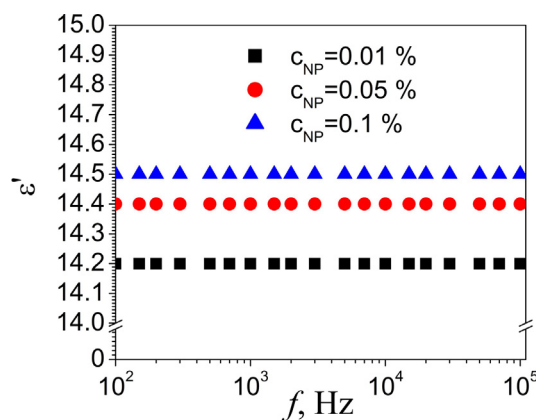

Fig. 1. Frequency dependences of the real part of the complex dielectric permittivity ε' for 6CB + 0.01 % wt/wt NP for three various sample thicknesses: 5 (1, squared times), 20 (2, red circles), and 50 μm (3, blue triangles). Temperature is 293 K (nematic phase of liquid crystal 6CB).

Fig. 2. Frequency dependence of the real part of the complex dielectric permittivity ε' in the region B measured for nematic liquid crystals 6CB doped with iron oxide nanoparticles of different weight concentration c_{NP}. The same values of ε' were obtained for cell thickness of 5, 20, and 50 μm. Temperature is 293 K (nematic phase of liquid crystals 6CB).

High frequency dispersion of ε' (region C) can be associated with the reorientation of a mesogenic molecule around its short axis [76]. In addition, in the case of thin cell (Fig. 1, squared times) parasitic effects caused by a finite resistance of ITO electrodes (~10 Ω/square) can also contribute to the observed high frequency dispersion of ε' [77,78].

While the real part of dielectric permittivity is independent of the cell thickness in the region B (10^2 – 10^5 Hz), both low frequency (<10^2 Hz, region B) and high frequency (>10^5 Hz, region C) dispersion of ε' becomes more pronounced for thinner cells (Fig. 1). Dielectric measurements performed at intermediate frequencies (10^2 – 10^5 Hz, region B) reveal information about bulk properties of nematic liquid crystals doped with nanoparticles. Experimental results presented in Fig. 1,2 also indicate that bulk dielectric (ε') measurements are independent of the cell thickness. As long as the alignment of liquid crystal samples is controlled, both thin and thick samples yield the same values of the real part of dielectric permittivity of liquid crystals doped with nanoparticles.

3.4. Frequency dispersion regions of the imaginary part of the complex dielectric permittivity.

In many practical cases, instead of the frequency dependence of the imaginary part of the complex dielectric permittivity ε'', it is more convenient to analyze the frequency dependence of the conductivity σ because the values of ε'' and σ are related according to Eq. (1). In this analysis, we excluded the low frequency region, and focused on intermediate (10^2-10^4 Hz) and high (>10^4 Hz) frequency ranges. The frequency dependences of the electrical conductivity of nematic liquid crystals 6CB doped with 0.01 % wt/wt nanoparticles measured using cells of three different thicknesses (5, 20, and 50 μm) are shown in Fig. 3.As can be seen from Fig. 3, the frequency dependence of the electrical conductivity exhibits two distinct regions that correspond to intermediate (10^2 – 10^4 Hz) and high (10^4 – 10^6 Hz) frequency ranges. In the case of intermediate frequency range, the observed frequency dependence of the electrical conductivity σ obeys Jonscher power law also known as the universal dielectric response [79] described by Eq. (4):

$$\sigma = \sigma_{DC} + Af^m \tag{4}$$

where σ_{DC} is the direct current (DC) electrical conductivity, f is the frequency, A and m are empirical parameters.

By applying Eq. (4) to experimental data (solid red curve, Fig. 3), the values of σ_{DC}, A and m can be evaluated. The first term of Eq. (4), DC electrical conductivity, is caused by ions present in liquid crystals doped with nanoparticles. The second term of Eq. (4) can be associated with electronic component of electrical conductivity. Ionic component of electrical conductivity dominates in the intermediate frequency range. Fig. 3 indicates that, for a given concentration of nanoparticles, the value of DC electrical conductivity depends on the cell thickness.

Similar behavior was observed for liquid crystals doped with higher concentrations of nanoparticles (Figs. 4 and 5).

Within an intermediate frequency range samples filled with nematic liquid crystals doped with low concentrations (0.01 % wt/wt and 0.05 % wt/wt) of nanoparticles show a very similar trend: the slope of a solid red curve decreases as a cell thickness goes up approaching a nearly zero value for a 50 μm thick cell (Figs. 3 and 4). This behaviour suggest that the ionic component of electrical conductivity is a dominant factor for thicker cells. For thinner cells we should also consider a contribution due to electronic conductivity of liquid crystals and nanoparticles. This contribution can be enhanced by a possible formation of chain-like aggregates of nanoparticles. The interactions between such
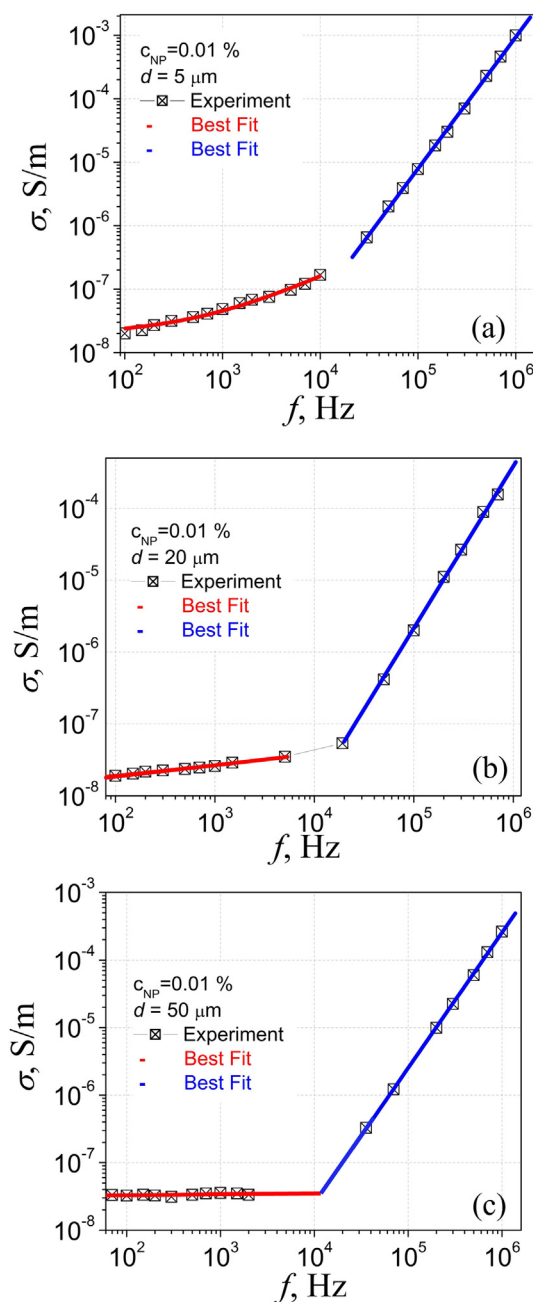

Fig. 3. Frequency dependence of electrical conductivity σ measured for nematic liquid crystals 6CB doped with 0.01 % wt/wt nanoparticles: (a) The cell thickness is 5 μm; (b) The cell thickness is 20 μm; and (c) The cell thickness is 50 μm. Temperature is 293 K.

chain-like aggregates can significantly increase the electronic component of the measured electrical conductivity of thinner cells (Fig. 3ab and Fig. 4ab). The applied electric field can facilitate the orientation of such chain-like nanoaggregates along the field that coincides with the direction of liquid crystal director. Thermal fluctuations can break such aggregates thus decreasing their contribution to the electrical conductivity of thicker samples. As a result, 50 μm thick cells exhibit nearly frequency independent electrical conductivity of ionic origin in the intermediate frequency range (Fig. 3c and 4c). It should be noted that further increase in the concentration of nanoparticles (0.01 wt%) results in a mixed electronic-ionic conductivity of the studied thin and thick samples (Fig. 5).
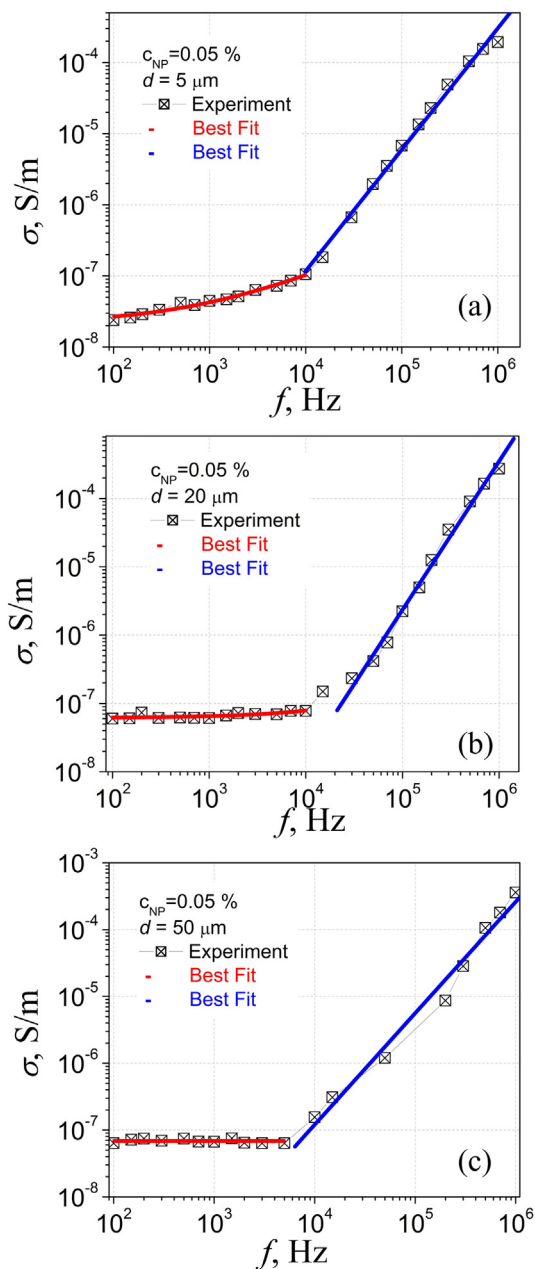
Fig. 4. Frequency dependence of electrical conductivity σ measured for nematic liquid crystals 6CB doped with 0.05 % wt/wt nanoparticles: (a) The cell thickness is 5 μm; (b) The cell thickness is 20 μm; and (c) The cell thickness is 50 μm. Temperature is 293 K.

Fig. 5. Frequency dependence of electrical conductivity σ measured for nematic liquid crystals 6CB doped with 0.1 % wt/wt nanoparticles: (a) The cell thickness is 5 μm; (b) The cell thickness is 20 μm; and (c) The cell thickness is 50 μm. Temperature is 293 K.

Experimental results shown in Fig. 3, Fig. 4, Fig. 5 unambiguously indicate that electrical conductivity of the studied samples depends on the concentration of nanoparticles and on the cell thickness. By applying Eq. (4) to experimental data obtained at intermediate frequencies ($10^2 – 10^4$ Hz), the values of σ_{DC}, A and m can be found. They are compiled in Table 1.

As was mentioned in the introduction section, the DC electrical conductivity is a very important parameter of liquid crystal materials. Table 1 can be used to analyze the dependence of the DC electrical conductivity of the studied samples on the concentration of nanoparticles and on the cell thickness. This dependence is shown in Fig. 6.

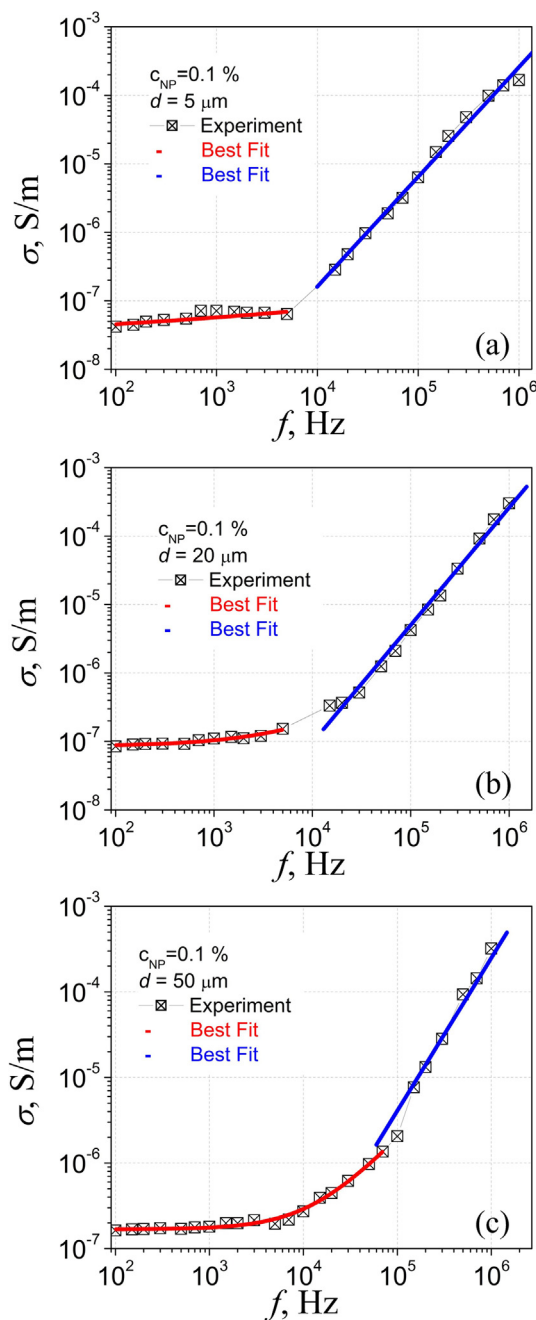As can be seen from Fig. 6a, the DC electrical conductivity of the studied samples increases as the concentration of nanoparticles increases. This increase is relatively weak for thin (5 μm) cells and becomes more pronounced if thicker (20 and 50 μm) cells are used (Fig. 6a). The observed increase in the DC electrical conductivity suggests that nanoparticles act as ion-generating objects. This behaviour is consistent with existing literature [63,64,80,81] and can be caused by several factors such as desorption and ionization of surfactants (oleic acid) stabilizing nanoparticles and/or by ionic contamination of nanodopants that occurred during their chemical synthesis and handling.

A very interesting result is the observed monotonous and non-monotonous dependence of the DC electrical conductivity of the studied samples on the cell thickness (Fig. 6b). A rather low concentration of nanoparticles (0.01 % wt/wt) in liquid crystals results

Table 1

The values of σ_{DC}, A and m obtained by applying Eq. (4) to experimental data measured for an intermediate frequency range (10^2–10^4 Hz).

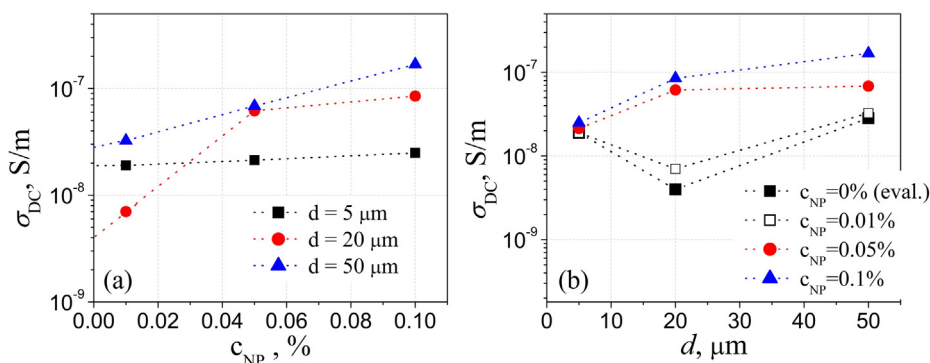| Cell	$c_{NP} = 0.01$ % wt/wt			$c_{NP} = 0.05$ % wt/wt			$c_{NP} = 0.1$ % wt/wt		
	σ_{DC}, S/m	A	m	σ_{DC}, S/m	A, $\frac{S}{ms^{-m}}$	m	σ_{DC}, S/m	A $\frac{S}{ms^{-m}}$	m
5 μm	1.900×10^{-8}	1.776×10^{-10}	0.725	2.126×10^{-8}	3.744×10^{-10}	0.585	2.492×10^{-8}	8.424×10^{-9}	0.195
20 μm	7.019×10^{-9}	4.427×10^{-9}	0.216	6.168×10^{-8}	3.369×10^{-11}	0.677	8.497×10^{-8}	1.030×10^{-10}	0.755
50 μm	3.249×10^{-8}	5.792×10^{-11}	0.479	6.840×10^{-8}	0	–	1.682×10^{-7}	2.546×10^{-12}	1.171

Fig. 6. The dependence of the DC (ionic) electrical conductivity σ_{DC} of nematic liquid crystals doped with nanoparticles on their weight concentration c_{NP} (a), and (b) on the cell thickness d.

in a non-monotonous (a decrease followed by an increase) dependence of the DC electrical conductivity on the cell thickness whereas larger nanodopant concentrations (0.05 and 0.1 % wt/wt) lead to a monotonous increase in the values of σ_{DC} (Fig. 6b). The observed dependence can be explained by considering the combined effect of nanoparticles and cell substrates on the concentration of ions in liquid crystal materials modelled in recent papers [66–68]. In the case of thin (5 μm) cells, the interactions between ions and substrates of the liquid crystal cell are dominant factors. The majority of ions generated by nanoparticles can get trapped by the substrates of the cell. As a result, the DC electrical conductivity exhibits a very weak dependence on the concentration of nanoparticles (Fig. 6ab). For intermediate values of the cell thickness (20 μm), the interactions between ions, substrates, and nanoparticles govern the DC electrical conductivity. Fig. 6 indicates that the ion capturing effect due to the substrates is still stronger than the ion releasing effect caused by low (0.01 % wt/wt) concentrations of nanoparticles in 20 μm thick liquid crystal cells. Further increase in the concentration of nanoparticles (0.05 and 0.1 % wt/wt) make ion releasing effect due to nanodopants dominate the ion capturing effect caused by the substrates of the cell. In the case of thick (50 μm) cells, the effect of interactions between ions and substrates on the DC electrical conductivity becomes insignificant. Thus, ion-generating properties of nanoparticles become a dominant factor that determines the values of the DC electrical conductivity of thick cells.

In the case of high frequency range (10^4–10^6 Hz), the dependence of the electrical conductivity σ on frequency f can be described by a power law (5):

$$\sigma = Bf^n \qquad (5)$$

where B and n are empirical parameters. The values of empirical parameters B and n were evaluated by applying Eq. (5) to experimental results (blue solid curves, Fig. 3, Fig. 4, Fig. 5). They are listed in Table 2.

Eq. (5) originates from relaxation phenomena due to the presence of mobile charge carriers of both electronic and ionic origin [79,82,83]. In addition, dispersion losses caused by dipolar relaxations and polarization processes originated from short range charge motions can also contribute to the AC conductivity [82,83]. Interestingly, while the DC conductivity of the studied samples strongly depends on both the concentration of nanoparticles and on the cell thickness (Fig. 6), the high frequency AC conductivity of the same samples is nearly independent of the nanoparticle concentration for intermediate (20 μm) and thick (50 μm) cells (Fig. 7). The results obtained for thin (5 μm) samples can be affected by the formation of nanoparticle clusters such as chains and molecular aggregates. This scenario can be realized if the interactions between nanoparticles are greater than the forces between liquid crystal molecules and nanodopants.

Experimental data shown in Fig. 7 suggests that the high-frequency electrical conductivity of the studied samples is caused by both free and bound ionic and electronic charge carriers in a liquid crystal host (major contribution) and it is nearly unaffected by nanodopants (for 20 μm and 50 μm thick cells). According to existing literature, the empirical parameter n of Eq. (5) can be related to the mechanisms of the conduction in the studied samples [79,82,83,84]. The obtained values of $n = 1.668 - 2.253$ (the super

Table 2

The values of parameters B and n obtained by applying Eq. (5) to experimental data measured for high frequency range (10^4–10^6 Hz).

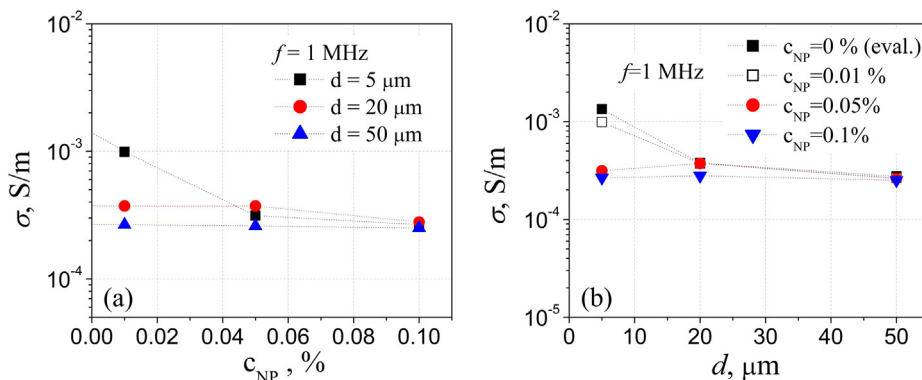| Cell	$c_{NP} = 0.01$ % wt/wt		$c_{NP} = 0.05$ % wt/wt		$c_{NP} = 0.1$ % wt/wt	
	B, $\frac{S}{ms^{-n}}$	n	B, $\frac{S}{ms^{-n}}$	n	B, $\frac{S}{ms^{-n}}$	n
5 μm	$10^{-15.467}$	2.073	$10^{-13.755}$	1.706	$10^{-13.197}$	1.602
20 μm	$10^{-16.933}$	2.253	$10^{-16.514}$	2.177	$10^{-13.875}$	1.742
50 μm	$10^{-15.631}$	2.006	$10^{-13.592}$	1.668	$10^{-14.314}$	1.785

Fig. 7. The dependence of the AC electrical conductivity σ_{DC} of nematic liquid crystals doped with nanoparticles on their weight concentration c_{NP} (a), and (b) on the cell thickness d. The frequency f is 1 MHz.

linear power law) overlap with recent experimental results reported for thermotropic compound 4-nonyloxy benzoic acid (9OBA) [85], nematic liquid crystal (E63) doped with nickel phthalocyanine [86], and nematic liquid crystals doped with diamond nanoparticles [87].

4. Conclusion

In this paper, we analysed the combined effect of the nanoparticle concentration and cell thickness on the dielectric and electrical properties of homeotropically aligned nematic liquid crystals. The dielectric spectra were measured within the $6 - 10^6$ Hz frequency range at room temperature (293 K).

We found that the frequency dependence of the real part of the complex dielectric permittivity ε' exhibits three regions, namely region A ($f < 10^2$ Hz), region B ($10^2 < f < 10^5$ Hz), and region C ($-10^5 < f < 10^6$ Hz) (Fig. 1). In the region A, the dispersion of ε' is caused by the near-electrode process and can be approximated by the Cole-Cole equation. This equation allowed to estimate the characteristic relaxation time (0.13 ± 0.10 s) and the thickness of the electrical double layers (150 ± 130 nm) for the sample "6CB + 0.1 wt% NP" of the thickness 50 μm. In the region B ($10^2 < f < 10^5$ Hz), the real part of the complex dielectric permittivity ε' does not depend on the frequency. It is also independent of the cell thickness (Fig. 1). In this region, bulk dielectric properties of the studied samples can be evaluated. The value of ε' can be tuned by changing the concentration of nanodopants (Fig. 2). A high frequency dispersion of ε' (region C, ($10^5 < f < 10^6$ Hz)) is caused by the reorientation of liquid crystalline molecules around its short axis. This observation agrees with existing literature [76]. In addition, a high frequency dispersion of ε' can also be the result of a parasitic effect related to ITO electrodes for thin cells [77,78].

To eliminate the effects caused by the electrode polarization, the electrical conductivity of the studied samples was analysed in the frequency range from 10^2 Hz to 10^6 Hz. It was found that in the frequency range from 10^2 Hz to 10^4 Hz the electrical conductivity of the studied samples obeys the Jonscher power law (Eq. (4)). The first term of Eq. (4) accounts for the direct current (DC) electrical conductivity, and the second term corresponds to the alternating current (AC) electrical conductivity. The DC electrical conductivity is caused by ions. By applying it to experimental data (red solid curves, Figs. 3-5), the values of the DC electrical conductivity σ_{DC} were found (Table 1). These values depend on the concentration of nanoparticles and on the cell thickness (Fig. 6, Table 1). The observed behaviour of σ_{DC} can be explained by considering the combination of ion capturing effect caused be the sub-

strates of the cell and ion releasing effect due to ionic contamination of nanoparticles. In the case of thin (5 μm) cells, the ion capturing effect dominates and, as a result, the dependence of the DC conductivity on the nanoparticle concentration is very weak. In other words, the effect of nanoparticles on the electrical properties of liquid crystals is "hidden". The use of thicker (50 μm) cells can reveal the true effect of nanoparticle on the DC electrical conductivity. For intermediate thicknesses (20 μm), the competition between the effect due to the substrates and the effect due to nanoparticles can result in an interesting non-monotonous dependence of the DC electrical conductivity on the cell thickness (Fig. 6b). This experimental finding has important practical implications. An experimental evaluation of the DC electrical conductivity of liquid crystal materials should involve samples of different thicknesses. This approach can also help to differentiate between the ionic effects caused by the substrates and by the nanoparticles. The alternating current (AC) electrical conductivity (the second term, Eq. (4)) in the studied frequency range can be attributed to the electronic conductivity due to nanodopants in liquid crystals. In the case of relatively thin cells, a formation of chains of nanoparticles can substantially contribute to the AC electrical conductivity.

In the frequency range from 10^4 Hz to 10^6 Hz the electrical conductivity of the studied samples can be described by a power law (5) and has a mixed, ionic-electronic origin.

Data availability

Data will be made available on request.

Declaration of Competing Interest

The authors declare that they have no known competing financial interests or personal relationships that could have appeared to influence the work reported in this paper.

Acknowledgements

References

[1] Y.J. Wang, Y.H. Lin, Liquid crystal technology for vergence-accommodation conflicts in augmented reality and virtual reality systems: a review, Liq. Cryst. Rev. 9 (1) (2021) 35–64, https://doi.org/10.1080/21680396.2021.1948927.

[2] J. Xiong, E.L. Hsiang, Z. He, T. Zhan, S.T. Wu, Augmented reality and virtual reality displays: emerging technologies and future perspectives, Light Sci. Appl. 10 (2021) 216.

[3] R. Morris, C. Jones, M. Nagaraj, Liquid Crystal Devices for Beam Steering Applications, Micromachines 12 (2021) 247, https://doi.org/10.3390/mi12030247.

[4] A.P.H.J. Schenning, G.P. Crawford, D.J. Broer (Eds.) Liquid crystal sensors, CRC Press, Taylor & Francis Group, Boca Raton, 12 (2018) 164 p.

[5] C. Jones, The fiftieth anniversary of the liquid crystal display, Liq. Cryst. Today 27 (3) (2018) 44–70, https://doi.org/10.1080/1358314X.2018.1529129.

[6] L.M. Blinov, Structure and Properties of Liquid Crystals, Springer, New York, NY, USA, 2010.

[7] K. Neyts, F. Beunis, Ion Transport in Liquid Crystals. In Handbook of Liquid Crystals: Physical Properties and Phase Behavior of 42 Liquid Crystals Chapter 11, Wiley-VCH, Weinheim, Germany, 2014, pp. 357–382.

[8] G. Barbero, L.R. Evangelista, Adsorption Phenomena and Anchoring Energy in Nematic Liquid Crystals, Taylor & Francis, Boca Raton, FL, USA, 2006.

[9] W. Lee, S. Kumar, Unconventional Liquid Crystals and Their Applications, De Gruyter, Berlin, Boston, 2021, 10.1515/9783110584370.

[10] J.P.F. Lagerwall, G. Scalia, (Eds.) Liquid Crystals with Nano and Microparticles; World Scientific: Singapore (2016). Volumes 2, ISBN 978-981-4619-25-7.

[11] Y. Shen, I. Dierking, Perspectives in Liquid-Crystal-Aided Nanotechnology and Nanoscience, Appl. Sci. 9 (2019) 2512.

[12] I. Dierking, From colloids in liquid crystals to colloidal liquid crystals, Liq. Cryst. 46 (2019) 2057–2074.

[13] J. Prakash, S. Khan, S. Chauhan, A.M. Biradar, Metaloxide-nanoparticles and liquid crystal composites: a review of recent progress, J. Mol. Liq. 297 (2020) 112052.

[14] P. Kopčanský, M. Timko, I. P. Studenyak, O. V. Kovalchuk, Nanoparticles in Homogenous, Micro- and Nanometric Structures Based on Liquid Crystals: Morphology and Dielectric Properties, Monograph. Košice, Institute of Experimental Physics, Slovak Academy of Sciences (2020).

[15] Y. Garbovskiy, Conventional and unconventional ionic phenomena in tunable soft materials made of liquid crystals and nano-particles, Nano Ex. 2 (2021) 012004.

[16] D.R. Evans et al., Inorganic Organic Photorefractive Hybrids, Springer International Publishing, Germany, 2016, pp. 223–247.

[17] Y. Chen et al., Soft optical metamaterials, Nano Convergence 7 (2020) 1–17.

[18] D.P.N. Gonçalves, M.E. Prévôt, Ş. Üstünel, T. Ogolla, A. Nemati, S. Shadpour, T. Hegmann, Recent progress at the interface between nanomaterial chirality and liquid crystals, Liq. Cryst. Rev. 9 (1) (2021) 1–34, https://doi.org/10.1080/21680396.2021.1930596.

[19] G. Klimusheva, T. Mirnaya, Y. Garbovskiy, Versatile nonlinear-optical materials based on mesomorphic metal alkanoates: design, properties, and applications, Liq. Cryst. Rev. 3 (1) (2015) 28–57, https://doi.org/10.1080/21680396.2015.1030461.

[20] Y. Garbovskiy, A. Glushchenko, Liquid crystalline colloids of nanoparticles: preparation, properties, and applications, Solid State Phys. 62 (2010) 1–74.

[21] A. Bukowczan, E. Hebda, K. Pielichowski, The influence of nanoparticles on phase formation and stability of liquid crystals and liquid crystalline polymers, J. Mol. Liq. 321 (2020) 114849.

[22] N. Tomašovicová, P. Kopcanský, N. Éber, Magnetically active anisotropic fluids based on liquid crystals Anisotropy Research: New Developments, Nova Science Pub Incorporated, USA, 2012, pp. 245–276.

[23] A. Mertelj, D. Lisjak, Ferromagnetic nematic liquid crystals, Liq. Cryst. Rev. (2017) 51–133.

[24] Y. Garbovskiy, A. Glushchenko, Ferroelectric nanoparticles in liquid crystals: recent progress and current challenges, Nanomaterials 7 (2017) 361.

[25] J. Mirzaei, M. Reznikov, T. Hegmann, Quantum dots as liquid crystal dopants, J. Mater. Chem. 22223 (2012) 50–65.

[26] S.G. Singh, Recent advances on cadmium free quantum dots-liquid crystal nanocomposites, Appl. Mater. Today 21 (2020) 100840.

[27] L. Dolgov, S. Tomylko, O. Koval'chuk, N. Lebovka, O. Yaroshchuk Liquid crystal dispersions of carbon nanotubes: dielectric, electro-optical and structural peculiarities Carbon Nanotubes, in: J.M. Marulanda (Eds.) (Croatia:Intech) 4 (2010) 51–84 (Chapter 24).

[28] S.P. Yadav, S. Singh, Carbon nanotube dispersion in nematic liquid crystals: an overview, Prog. Mater. Sci. 80 (2016) 38–76.

[29] A. Choudhary et al., Advances in gold nanoparticle–liquid crystal composites, Nanoscale 677 (2014) 43–56.

[30] Y.C. Hsiao, S.M. Huang, E.R. Yeh, W. Lee, Temperature dependent electrical and dielectric properties of nematic liquid crystals doped with ferroelectric particles, Displays 44 (2016) 61–65.

[31] S. Al-Zangana, M. Turner, I. Dierking, A comparison between size dependent paraelectric and ferroelectric $BaTiO_3$ nanoparticle doped nematic and ferroelectric liquid crystals, J. Appl. Phys. 121 (2017) 085105.

[32] P. Kumar, S. Debnath, N.V. Rao, A. Sinha, Nanodoping: a route for enhancing electro-optic performance of bent core nematic system, J. Phys. Condens. Matter 30 (2018) 095101.

[33] S. Lalik et al., Modification of AFLC physical properties by doping with $BaTiO_3$ particles, J. Phys. Chem. B 124 (2020) 6055–6073.

[34] M.B. Salah, R. Nasri, A.N. Alharbi, T.M. Althagafi, T. Soltani, Thermotropic liquid crystal doped with ferroelectric nanoparticles: Electrical behavior and ion trapping phenomenon, J. Mol. Liq. 357 (2022), https://doi.org/10.1016/j.molliq.2022.119142 119142.

[35] A. Parveen, J. Prakash, G. Singh, Impact of strontium titanate nanoparticles on the dielectric, electro-optical and electrical response of a nematic liquid crystal, J. Mol. Liq. 354 (2022), https://doi.org/10.1016/j.molliq.2022.118907 118907.

[36] D. Varshney, Anu, J. Prakash, V.P. Singh, K. Yadav, G. Singh, Probing the impact of bismuth-titanate based nanocomposite on the dielectric and electro-optical features of a nematic liquid crystal material, J. Mol. Liq. 347 (2022) 118389, https://doi.org/10.1016/j.molliq.2021.118389.

[37] I.P. Studenyak, O.V. Kovalchuk, S.I. Poberezhets, M.M. Luchynets, A.I. Pogodin, M. Timko, P. Kopčanský, Electrical conductivity of composites based on 6CB liquid crystal and $(Cu_6PS_5I)_{0.5}(Cu_7PS_6)_{0.5}$ superionic nanoparticles, Mol. Cryst. Liq. Cryst. 718 (1) (2021) 92–101, https://doi.org/10.1080/15421406.2020.1861526.

[38] S.I. Poberezhets, O.V. Kovalchuk, I.P. Studenyak, T.M. Kovalchuk, I.I. Poberezhets, V. Lacková, M. Timko, P. Kopčanský, Temperature dependence of dielectric properties of the liquid crystal 6CB with the embedded Ag_7GeS_5I nanoparticles, Semiconductor Phys. Quantum Electron. 23 (2) (2020) 129–135, https://doi.org/10.15407/spqeo23.02.129.

[39] V.E. Vovk, O.V. Kovalchuk, P. Kopčanský, T.M. Kovalchuk, Dielectric properties of nematic liquid crystal with impurities of supramolecular Ni-TMTAA-TCNQ complexes, Semiconductor Phys. Quantum Electron. 23 (2) (2020) 146–154, https://doi.org/10.15407/spqeo23.02.146.

[40] S. Kredentser, S. Tomylko, T. Mykytiuk, et al., Electro-optical properties of a liquid crystal line colloidal solution of rod shaped V2O5 nanoparticles and carbon nanotubes in an alternating current electric field, Liq. Cryst. 48 (14) (2021) 2027–2034, https://doi.org/10.1080/02678292.2021.19199337.

[41] S. Tomylko et al., Structural evolution and dielectric properties of suspensions of carbon nanotubes in nematic liquid crystals Phys, Chem. Chem. Phys. 19 (2017) 16456–16463.

[42] M.C. Cetinkaya et al., The effect of –COOH functionalized carbon nanotube doping on electro-optical, thermo-optical and elastic properties of a highly polar smectic liquid crystal, J. Mol. Liq. 272 (2018) 801–814.

[43] I.P. Studenyak, P. Kopčanský, M. Timko, M. Mitroova, O.V. Kovalchuk, Effects of non-additive conductivity variation for a nematic liquid crystal caused by magnetite and carbon nanotubes at various scales, Liq. Cryst. 44 (2017) 1709–1716.

[44] R.K. Shukla, A. Chaudhary, A. Bubnov, K.K. Raina, Multiwalled carbon nanotubes-ferroelectric liquid crystal nanocomposites: effect of cell thickness and dopant concentration on electro-optic and dielectric behaviour, Liq. Cryst. 45 (2018) 1672–1681.

[45] A. Debnath, P.K. Mandal, Influence of carbon nanotubes on the dielectric and electro-optical properties of a proto-type ferroelectric mixture used in display devices, J. Mol. Liq. 343 (2021), https://doi.org/10.1016/j.molliq.2021.117653 117653.

[46] P.J. Jessy, S. Radha, P. Nainesh, Highly improved dielectric behaviour of ferronematic nanocomposite for display application, Liq. Cryst. 46 (2019) 772–786.

[47] F.P. Pandey, A. Rastogi, R. Manohar, R. Dhar, S. Singh, Dielectric and electro-optical properties of zinc ferrite nanoparticles dispersed nematic liquid crystal 4'-Heptyl-4-biphenylcarbonnitrile, Liq. Cryst. 47 (2020) 1025–1040.

[48] G. Kaur, Khushboo, P. Malik, Mesomorphic, electro-optic and dielectric behavior of self-assembled nanocomposite materials: Nematic mixture doped with carbon coated cobalt nanoparticles, J. Mol. Liq. 351 (2022), https://doi.org/10.1016/j.molliq.2022.118639 118639.

[49] D.K. Gaur, F.P. Pandey, A. Rastogi, et al., Investigation of dielectric, optical and zeta potential properties of pure and zinc ferrite nanoparticles dispersed nematic liquid crystal PCH5, Appl. Phys. A 128 (2022) 230, https://doi.org/10.1007/s00339-022-05318-1.

[50] E. Konshina, D. Shcherbinin, M. Kurochkina, Comparison of the properties of nematic liquid crystals doped with TiO_2 and CdSe/ZnS nanoparticles, J. Mol. Liq. 267 (2018) 308–314.

[51] H. Ayeb, S. Alaya, M. Derbali, L. Samet, J. Bennaceur, F. Jomni, T. Soltani, Dielectrical, electro-ptical and textural studies of 5CB nematic liquid crystal doped with TiO_2 and $Cu-TiO_2$ nanoparticle, Liq. Cryst. 48 (2) (2021) 223–232, https://doi.org/10.1080/02678292.2020.1771784.

[52] G. Kaur, P. Kumar, A.K. Singh, D. Jayoti, P. Malik, Dielectric and electro-optic studies of a ferroelectric liquid crystal dispersed with different sizes of silica nanoparticles Liq, Cryst. 47 (2020) 2194–2208.

[53] A. Rani, S. Chakraborty, A. Sinha, Effect of CdSe/ZnS quantum dots doping on the ion transport behavior in nematic liquid crystal, J. Mol. Liq. 342 (2021), https://doi.org/10.1016/j.molliq.2021.117327 117327.

[54] A. Rastogi, P.K. Tripathi, T. Manohar, R. Manohar, Dielectric and electro-optical properties of nematic liquid crystal p-methoxybenzylidene p-decylaniline dispersed with oil palm leaf based porous carbon quantum dots, J. Dispersion Sci. Technol. (2021), https://doi.org/10.1080/01932691.2021.1981366.

[55] A.D. Kurilov, D.N. Chausov, V.V. Osipova, R.N. Kucherov, V.V. Belyaev, Y.G. Galyametdinov, Highly luminescent nanocomposites of nematic liquid crystal and hybrid quantum dots CdSe/CdS with ZnS shell, J. Mol. Liq. 339 (2021), https://doi.org/10.1016/j.molliq.2021.116747 116747.

[56] F.V. Podgornov, M. Gavrilyak, A. Karaawi, V. Boronin, W. Haase, Mechanism of electrooptic switching time enhancement in ferroelectric liquid crystal/gold nanoparticles dispersion Liq, Cryst. 45 (2018) 1594–1602.

[57] R. Katiyar et al., Silver nanoparticles dispersed in nematic liquid crystal: an impact on dielectric and electro-optical parameters, J. Theor. Appl. Phys. 14 (2020) 237–243.

[58] D.N. Chausov et al., Electro-optical performance of nematic liquid crystals doped with gold nanoparticles, J. Phys. Condens. Matter 32 (2020) 395102.

[59] J.R. Macdonald, Impedance Spectroscopy, Emphasizing Solid Materials and Systems, John Wiley & Sons, New York, NY, USA, 1987, p. 368.

[60] A. Sawada, K. Tarumi, S. Naemura, Novel characterization method of ions in liquid crystal materials by complex dielectric constant measurements, Jpn. J. Appl. Phys. 38 (1999) 1423–1427, https://doi.org/10.1143/jjap.38.1423.

[61] A.V. Kovalchuk, Relaxation processes and charge transport across liquid crystals – electrode interface, J. Phys.: Condensed Matter. 13 (24) (2001) 10333–10345, https://doi.org/10.1088/0953-8984/13/46/306.

[62] A.R. Karaawi, M.V. Gavrilyak, V.A. Boronin, A.M. Gavrilyak, J.V. Kazachonok, F.V. Podgornov, Direct current electric conductivity of ferroelectric liquid crystals–gold nanoparticles dispersion measured with capacitive current technique, Liq. Cryst. 47 (2020) 1507–1515.

[63] S. Tomylko, O. Yaroshchuk, O. Kovalchuk, U. Maschke, R. Yamaguchi, Dielectric properties of nematic liquid crystal modified with diamond nanoparticles, Ukrainian J. Phys. 57 (2012) 239–243.

[64] Y. Garbovskiy, Switching between purification and contamination regimes governed by the ionic purity of nanoparticles dispersed in liquid crystals, Appl. Phys. Lett. 108 (2016) 121104.

[65] Y. Garbovskiy, Nanomaterials in liquid crystals as ion-generating and ion-capturing objects, Crystals 8 (2018) 264, https://doi.org/10.3390/cryst8070264.

[66] Y. Garbovskiy, Ion capturing/ion releasing films and nanoparticles in liquid crystal devices, Appl. Phys. Lett. 110 (2017) 041103.

[67] Y. Garbovskiy, Ions and size effects in nanoparticle/liquid crystal colloids sandwiched between two substrates. The case of two types of fully ionized species, Chem. Phys. Lett. 679 (2017) 77–85.

[68] Y. Garbovskiy, Kinetics of ion-capturing/ion-releasing processes in liquid crystal devices utilizing contaminated nanoparticles and alignment films, Nanomaterials 8 (2018) 59.

[69] O.V. Kovalchuk, Adsorption of ions and thickness dependence of conductivity in liquid crystal, Semicond. Phys. Quantum Electron. Optoelectron. 14 (2011) 452–455.

[70] D. Webb, Y. Garbovskiy, Overlooked ionic phenomena affecting the electrical conductivity of liquid crystals, Eng. Proc. 11 (2021) 1, https://doi.org/10.3390/ASEC2021-11141.

[71] S. Dhara, N.V. Madhusudana, Ionic contribution to the dielectric properties of a nematic liquid crystal in thin cells, J. Appl. Phys. 90 (2001) 3483–3488.

[72] A. Kumar, D. Varshney, J. Prakash, Role of ionic contribution in dielectric behaviour of a nematic liquid crystal with variable cell thickness, J. Mol. Liq. 303 (2020) 112520.

[73] K. Zakutanská, D. Petrov, P. Kopčanský, D. Węgłowska, N. Tomašovičová, Fréedericksz transitions in 6CB based ferronematics—Effect of magnetic nanoparticles size and concentration, Materials 14 (2021) 3096, https://doi.org/10.3390/ma14113096.

[74] G.W. Gray, K.J. Harrison, J.A. Nash, New family of nematic liquid crystals for displays, Electron Lett. 9 (1973) 130–131, https://doi.org/10.1049/el:19730096.

[75] A.J. Twarowski, A.C. Albrecht, Depletion layer studies in organic films: Low frequency capacitance measurements in polycrystalline tetracene, J. Chem. Phys. 70 (1979) 2255–2261, https://doi.org/10.1063/1.437729.

[76] W. Haase, S. Wróbel (Eds.). Relaxation Phenomena. Liquid Crystals, Magnetic Systems, Polymers, High-Tc Superconductors, Metallic Glasses. Springer-Verlag Berlin Heidelberg (2003) 10.1007/978-3-662-09747-2.

[77] P. Perkowski, The parasitic effects in high-frequency dielectric spectroscopy of liquid crystals – the review, Liq. Cryst. 48 (6) (2021) 767–793, https://doi.org/10.1080/02678292.2020.1852619.

[78] R. Dhar, An impedance model to improve the higher frequency limit of electrical measurements on the capacitor cell made from electrodes of finite resistances, Ind. J. Pure Appl. Phys. 42 (2004) 56–61.

[79] A.K. Jonscher, The 'universal' dielectric response, Nature 267 (1977) 673–679.

[80] M. Urbanski, J.P.F. Lagerwall, Why organically functionalized nanoparticles increase the electrical conductivity of nematic liquid crystal dispersions, J. Mater. Chem. C 5 (2017) 8802–8809.

[81] Y. Garbovskiy, On the analogy between electrolytes and ion-generating nanomaterials in liquid crystals, Nanomaterials 10 (2020) 403, https://doi.org/10.3390/nano10030403.

[82] J.C. Dyre, T.B. Schrøder, Universality of ac conduction in disordered solids, Rev. Mod. Phys. 72 (2000) 873–892, https://doi.org/10.1103/RevModPhys.72.873.

[83] C. Tsonos, Comments on frequency dependent AC conductivity in polymeric materials at low frequency regime, Curr. Appl. Phys. 19 (4) (2019) 491–497, https://doi.org/10.1016/j.cap.2019.02.001.

[84] Ş. Özğan, H. Eskalen, Y. Tapkıranlı, The electrical and optical behavior of graphene oxide-doped nematic liquid crystal, J Mater Sci: Mater Electron 33 (2022) 5720–5729, https://doi.org/10.1007/s10854-022-07758-0.

[85] S. Patari, A. Nath, Frequency tuned dielectric and electrical properties of a thermotropic liquid crystal compound 9OBA, Mater. Today: Proc. 5 (1, Part 2) (2018) 2105–2111, https://doi.org/10.1016/j.matpr.2017.09.207.

[86] M. Kılıç, Z.G. Özdemir, N.Y. Canli, A.E. Bulgurcuoğlu, O. Köysal, Ö. Yılmaz, M. Okutan, The impact of NiPc additive and laser light dielectric properties of E63 nematic liquid crystal, Ferroelectrics 505 (1) (2016) 102–113, https://doi.org/10.1080/00150193.2016.1254586.

[87] A. Barrera, C. Binet, F. Dubois, P.-A. Hébert, P. Supiot, C. Foissac, U. Maschke, Dielectric spectroscopy analysis of liquid crystals recovered from end-of-life liquid crystal displays, Molecules 26 (2021) 2873, https://doi.org/10.3390/molecules26102873.